International Journal of GEOMATE, April, 2025 Vol.28, Issue 128, pp.19-32
ISSN: 2186-2982 (P), 2186-2990 (O), Japan, DOI: https://doi.org/10.21660/2025.128.4654
Geotechnique, Construction Materials and Environment

COASTAL SAFETY STRUCTURE PLANNING USING MODIFICATION OF ARTIFICIAL FISH APARTMENTS AT NORTH JAVA COASTAL INDONESIA

*Widyaningtias[1], Geryan Hardianto Putra[1], Ingerawi Sekaring Bumi[2], Aris Ismanto[3], Mohammad Bagus Adityawan[1], Arno Adi Kuntoro[1], Donny Rizki Pratama Santosa[1]

[1]Study Program of Water Resources Engineering and Management, Faculty of Civil and Environmental Engineering, Institut Teknologi Bandung, Indonesia
[2]Waterworks Construction Technology, Politeknik Pekerjaan Umum, Indonesia
[3]Integrated Coastal Zone Management Laboratory, Universitas Diponegoro, Indonesia

*Corresponding Author, Received: 26 July 2024, Revised: 11 Dec. 2024, Accepted: 13 Dec. 2024

ABSTRACT: Indonesia is in the spotlight due to erosion and abrasion, especially on the North Coast of Java. The location of Tirang Beach, which is part of the North Java coast, has faced these problems for a few years. This disaster is also aggravated by the rising sea level caused by climate change. Tirang Beach area requires restoration efforts to improve the quality of life for the community. Artificial Fish Apartment (AFA) is proposed as a coastal protection alternative. This structure is designed to catch sediment, restore the marine ecosystem's habitat, and be a tourist attraction. The AFA structure will consist of concrete blocks with cavities on each side of the block. The concrete block is square and arranged stacked up to resemble a trapezoid. The modelling of hydrodynamic and sediment transport conditions using Delft3D models was carried out. Modelling is conducted for three AFA layout scenarios and compared to existing conditions. The study indicates that scenario two positively impacts the emergence of new land. The analysis shows that scenario two gets maximum sedimentation and is the most significant change for the seabed elevation change. Thus, it is predicted that reaching MSL will take approximately four years. Compared to the existing condition, the average calculated wave height reduction is approximately 0.3 m. The Analytic Hierarchy Process (AHP) method was employed to determine the best alternatives. The results indicate that scenario two is highly recommended as the top priority, followed by scenario 5 in second place.

Keywords: Coastal restoration, Erosion, Artificial fish apartment, Hydrodynamic modelling, Sediment transport

1. INTRODUCTION

Indonesia, is a nation of interconnected islands [1], is rich in territorial waters and natural resources. Its diverse marine life, including fish, shrimp, and seaweed, is a shared treasure that must be preserved for the benefit of all Indonesians. This interconnectedness underscores the shared responsibility in maintaining the sustainability of our marine resources [2].

Indonesia's island-dotted geography results in a vast expanse of seas and coastal areas, which are often the heart of our activities [3]. For many Indonesians, particularly those who make a living as fishermen, these waters are not just a source of life but a lifeline. The marine potential for our communities is not just significant; it's urgent and must be harnessed for the sustainability of our society.

Since a few years ago, the coasts over the world have faced a lot of issues related to coastline change, such as in South Africa [4], Southeast Asia [5], and Australia [6]. This problem also happened in Indonesia [7]. There are some causes of this phenomenon, such as erosion and abrasion [8], land degradation [9], climate change [10], sea level rise [11] and land subsidence [12]. From all the causes, the common problems take place around the world through erosion and abrasion [13]. Erosion and abrasion happen because of the sea waves from the deep seas. The climate change [14] and sea level rise [15] increase the number of locations affected by erosion and abrasion.

Erosion of coastal areas due to waves and ocean currents, as well as abrasion, a natural process in the form of soil erosion or rocks, can significantly impact the marine ecosystem [16]. The sediments carried by the sea can damage the coastline, affecting the habitats of marine life. These two processes can harm nature and humans living in the vicinity area and disrupt the delicate balance of the ecosystem.

The disaster will impact the retreat in the community's economic sector and will continue to impact the community's welfare [17]. Many people will lose their homes because the land area has experienced erosion and seawater abrasion [14]. Therefore, the sustainability and defence of Indonesia's coastline are essential, and a solution is needed to address the problems in Indonesia.

In Indonesia, many coastline areas are experiencing deterioration, especially Semarang, the north coast of Java [18]. Along the coastline, there are many tourist attractions, such as pond fish farming and residences around the area. The main problems at

Semarang Beach are erosion and abrasion due to destructive waves that keep the coastline retreating [19].

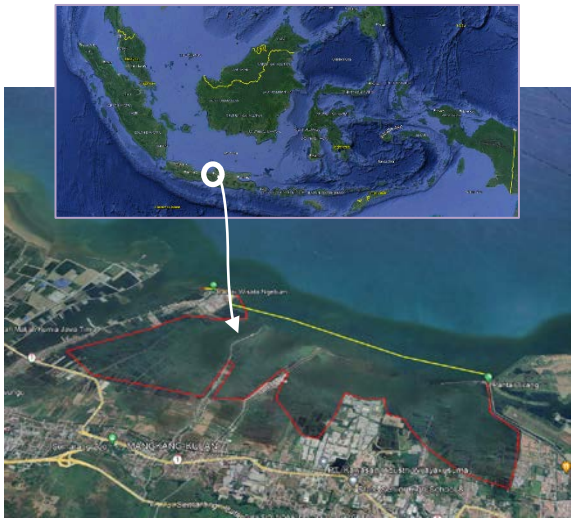

Fig. 1 Location of Tirang Beach, in 2023 (red line) and 1985 (yellow line) coastal line

Figure 1 shows the location of Tirang Beach. The yellow line shows the coastline in 1985, and the red one shows the coastline in 2023. This picture shows massive erosion and abrasion in this area for over 30 years. The coastline has moved up to 2 km from the initial, and much land has gone.

According to personal digitization, the coastline of Tirang has retreated around 2,500 m for 38 years. Thus, Tirang Beach's coastline has retreated about 65 m every year. Tirang Island, previously a mainland area, now only remains of beach sand.

The retreat in the coastline is not simultaneous [20]. A long erosion process occurred continuously to form a bowl, which became like a bay. Therefore, a solution design plan will be carried out to overcome the problem of shoreline retreat in Central Java. A breakwater structure can probably prevent erosion and abrasion on the north coast of Java.

The design plan is at Tirang Beach, North Java Coastal, Indonesia. This structure was chosen since Tirang Beach is a tourist location, and it can reduce wave energy [21] while still paying attention to environmental aspects [22]. Fish farming can also be done in the area. It will be below the water's surface and will not detract from the beach waters and the scenery.

2. RESEARCH SIGNIFICANCE

The breakwater is designed using a permeable structure. Permeable structure is porous structure that allows water to pass the structure while others are reflected. The structure that will be designed is a kind of artificial reef called an Artificial Fish Apartment (AFA). The structure is used to reduce sea waves partially [23]**,** rebuilds marine aquatic ecosystems [24]**,** and also trap sediment at the back of the structure. In a few years, the AFA's structure will be new habitat for marine ecosystem and the sediments will gradually become land again to restore the beach to its original shape [25].

3. MATERIALS AND METHODS

3.1 Wave Reflection

Wave reflection is a change in the direction of wave propagation towards the medium of origin (reflected) when it hits a barrier. The law of wave reflection is that the angle of the incidence of the wave is equal to the angle of the reflection of the wave. Incoming waves that hit an obstacle will be partially or wholly reflected [26]. Reviewing wave reflection is essential in planning coastal structures, especially coastal construction. Table 1 shows a comparison between dam type and its reflection coefficient (Kr).

$$Kr = \frac{Hr}{Hi} = \left(\frac{Er}{Ei}\right)^{0.5} \quad (1)$$

Table 1. Reflection Coefficient Based on Structure Type

DAM Type	Kr
Vertical wall with a peak above the water	0.7 – 1.0
Vertical wall with submerged top	0.5 – 0.7
Slanted-sided stone pile	0.3 – 0.6
Pile of concrete blocks	0.3 – 0.5
(perforated)	0.05 – 0.2

A structure that has sloping sides and is made of piles of stones will be able to absorb more wave energy than an upright and massive structure. When incoming waves meet or encounter obstacles such as coastal defence structures, these waves are wholly or partially reflected [26]. The event of a reflected wave that hits an obstacle is called a reflected wave. Wave reflection influences the wave vicinity [27]. The reflection factor can be formulated as Eq. (1), or we can use the number of Kr instantly, as shown in the Table 1.

Wave reflection analysis is critical in designing coastal defense structures because it determines whether the structure can optimally absorb wave energy [28]. The reflection coefficient, which is the ratio between the reflected or reflected wave height and the incident wave height, can determine the structure's ability to reflect waves.

3.2 Wave Transmission

Wave transmission is the remaining energy of a

wave after passing through/penetrating a wave barrier structure. Wave characteristics highly influence the transmission of waves. The transmission coefficient (t) is the ratio of the amplitude of the transmitted wave to the incoming wave. Wave transmission occurs when a structure partially blocks high waves but not entirely, allowing the remaining wave to communicate towards the shore. The emitted wave height is smaller than the incoming wave and the wave period, which differs in magnitude. Considering irregular waves, the transmission coefficient is the ratio or proportion between the wave height passing through the structure and the incoming wave height, obtained from Eq. (2).

$$Kt = \frac{Ht}{Hi} = \left(\frac{Et}{Ei}\right)^{0.5} \quad (2)$$

The Simulating Waves Near Shore (SWAN) model in the Delft3D-Wave menu can estimate wave transmission through structures such as underwater structures acting as Artificial Fish Apartments (AFA) in this study. However, the equation does not include the structure's porosity parameter. Therefore, the AFA structure is modelled using an obstacle feature barrier with a type adapted to its shape from its cross-section.

$$Kt_{submerged} = 0.5\left(1 - sin\left(\frac{\pi}{2\alpha}\left(\frac{Rc}{Hi} + \beta\right)\right)\right) \quad (3)$$

With

$$-\beta - \alpha < \frac{Rc}{Hi} < \alpha - \beta \quad (4)$$

In determining the transmission coefficient values of the embedded structure for each modelling scenario, they need to be found using previous calculations to be included in the wave modelling parameters as shown in Eq. (3). The equation used when the value of α and β meet the Eq. (4). A more straightforward way, coefficient α and β for the structure type coefficients based on the Seelig coefficient based on Delft3D-flow user manual has listed in Table 2.

Table 2. Reflection Coefficient Based on Structure Type

Case Type of Obstacle	α	β
Vertical Thin Wall	1.8	0.1
Caisson	2.2	0.4
Dam with slope 1 : $\frac{3}{2}$	2.6	0.15

3.3 Wave Hindcasting

The wave hindcasting was conducted to determine the significant wave height (Hs), wave period (Tp) and wave direction. Waves are complex phenomena formed due to long-term wind and happen continuously [29]. Hence, the wave was influenced by the wind stress factor (Ua) and effective fetch length (Feff). The data was formulated using numerical simulation. The wind stress factor is the strength of the wind blowing, while fetch indicates the wind races in 8 directions. Wave hindcasting was analyzed for each direction.

3.4 Hydrodynamic Modeling

Deltares has developed fully integrated computer software encompassing various multidisciplinary approaches and 2D computations for coastal, river, and estuarine areas. The simulations using Navier Stoke Equation that can be performed include water flow, sediment transport, waves, water quality, morphological development, and ecology [30].

This model is a hydrodynamic simulation program that calculates non-steady flow and transport phenomena due to tidal and meteorological forces acting on a square or curved longitude-latitude grid [31]. Several input files are required when setting up the hydrodynamic model in Delft3D. These files are crucial for modelling the Artificial Fish Apartment structure and include data on tide, wind, topography, sediment concentration, and estuarine sediment concentration and discharge [32].

4. RESULTS AND DISCUSSION

This research utilizes software to model the occurrence of currents and waves using Delft3D-Flow and Delft3D-Wave, which will be coupled to obtain accurate modelling results. Additionally, the sedimentation and erosion data will be examined at several designated observation points, further explained in the following section.

4.1 Fetch Processing

The fetch processing serves as an input parameter for hindcasting to determine wave height and period. This allows for visualization of the directions from which waves will approach Tirang Beach. The fetch is created using AutoCAD software, incorporating a map of Indonesia. The fetch follows the SPM 1984 standard, with points located 20 m from the shoreline as the central point. From these points, lines are drawn at a maximum of 120 km or until the fetch line reaches an obstacle. There are 72 fetch lines at every 5-degree angle. The formula for calculating the effective fetch is in Eq. (5).

$$F_{eff} = \frac{\sum Fi * cos\alpha}{\sum \cos\alpha} \quad (5)$$

The calculation results are presented in Figure 2 and Table 3. As a result, each cardinal direction has

nine fetch lines; each indicated with a different colour. Every colour shows a different direction of fetch. Each fetch's length and angle data are recorded to calculate Hs and Ts. Therefore, from the effective fetch lengths calculated, it can be observed that the most extended and dominant effective fetch length is from the northwest direction, with a length of 120,000 m.

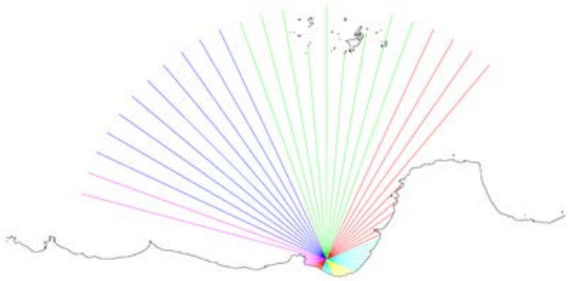

Fig. 2 Fetch Analysis

Table 3. Table of Fetch Calculation Results

Direction	Length (m)
North	114,025
North East	74,453
East	19,625
South East	11,025
South	6,282
Southwest	5,775
West	34,097
Northwest	120,000

4.2 Significant Wave Height and Period

Calculated of Hs (significant wave height) and Ts (significant wave period) using the corrected wind data. One of the corrections involves adjusting the U(10) elevation. This correction is necessary because the wind data collected from NOAA is surface wind data obtained from a layer in the atmosphere known as the constant shear layer. The wind is located within a height up to 10 m above sea level. The wind data is adjusted to a height of 10 m based on the wind observation speed rate. The wind stress factor (Ua) is calculated using the Eq. (6) formula.

$$Ua = 0.71 (U10)1.23. \quad (6)$$

After the initial calculations, further analyses were conducted to determine the significant wave height and period for each direction. This involved classifying the data for each direction to identify the highest and most dominant Hs and Ts values. The influence of fetch lengths on these values is significant, with the most extended fetch lengths unobstructed by land masses, resulting in the most dominant and more substantial wave height and period. Therefore, calculations for significant waves and periods were generated for the eight designated directions according to the fetch divisions. The resulting calculations for Hs and Ts are as follows in Table 4.

Table 4. Recapitulation of Hs and Ts in 8 Directions

Direction	Hs (m)	Ts (s)
North	0.59	3.79
North East	0.35	2.80
East	0.36	2.53
South East	0.23	2.03
South	0.13	1.55
Southwest	0.13	1.51
West	0.33	2.63
Northwest	0.91	2.92

Based on the analysis, the wave forecasting conducted shows that the most dominant waves are observed from the North and Northwest directions. This is supported by the considerable fetch lengths due to the absence or minimal obstruction from land masses. The dominant waves from the North direction have a significant wave height (Hs) of 0.6 m and a considerable wave period (Ts) of 3.8 s, and from the Northwest, the wave reaches 0.91 m (Hs) and period 2.92 s (Ts).

4.3 Existing Condition

All the data collected is used as input data in the Delft3D model. For the first condition, we create a model in the existing condition. This model aims to forecast the condition of Tirang Beach three months later. There are 25 observation points as shown with x mark. Observation points were added around the coastline to get information. Figure 3 represents the observation points in the red box from T1 until T25.

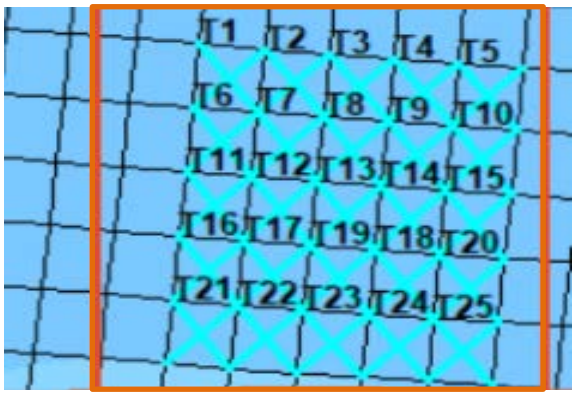

Fig. 3 Observation Points

As predicted, the modelling results for the next three months indicate a significant and continuous erosion, leading to a substantial decrease in the seabed's surface level. Figure 4, a sample from 4 of the 25 observation points, shows the cumulative

erosion over time. The highest erosion occurs in the first month and continues until the third month, with the cumulative erosion for three months reaching almost 0.05 m. This continuous erosion brings negative implications to the coastal area.

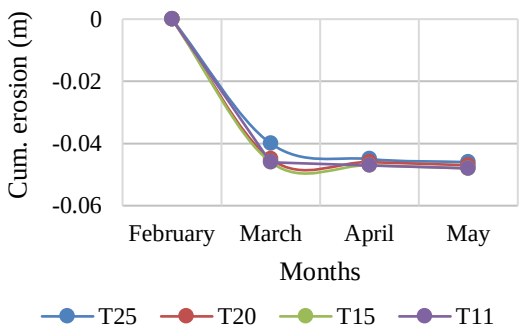

Fig. 4 Cumulative Erosion

4.4 Safety Structure Scenarios for Tirang Beach

The planning of the AFA (Artificial Fish Apartment) structure will involve several scenarios that will be further analysed to determine the most effective solution with the most positive impact on the erosion events. The purpose is to achieve the maximum erosion reduction or even transform the existing erosion conditions into significant sedimentation, Since waves from the Northwest direction predominantly influence Tirang Beach, it is estimated that the structure, in addition to being parallel to the shoreline, should be designed perpendicular to the coast to effectively reduce wave impact and maximise sediment trapping behind the structure.

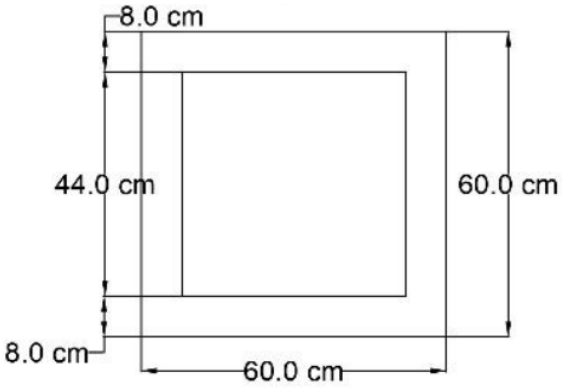

Fig. 5 Detail Dimension of Artificial Fish Apartment

The modified AFA structure will consist of concrete blocks arranged in a specific pattern with cavities on the sides of each block. The concrete block has a square shape with a side length of 60 cm in the outer and 44 cm in the inner as visualise in 2D at Figure 5. The structure is arranged in a stacked up to resemble a trapezoid, as seen in the Fig. 6.

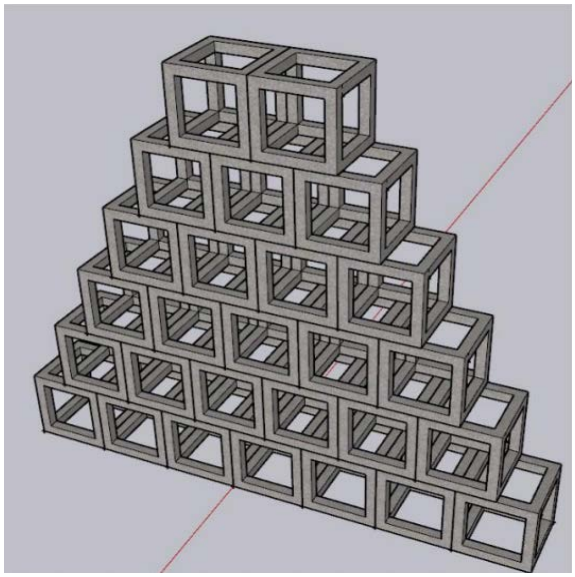

Fig. 6 Structure of Artificial Fish Apartment

The focus of the research is finding the best layout configuration of the AFA's structure; hence, three scenarios are proposed. Every scenario is designed with distinct configurations, as shown with the orange colour in Fig. 7. The size of the scenario designs follows the dimensions of the grid, which is square with 50 m x 50 m in length.

4.4.1 Scenario 1

The first scenario of the AFA structure was arranged vertically up to 1.8 m. It was located around 100 m from the coastline and designed like a T-shaped structure, as shown in the red line in Figure 6. The length of the T-shaped structure is 150 m and 100 m**.**

4.4.2 Scenario 2

The second scenario of the AFA structure is designed like a square temple. This structure consists of two layers with different lengths and heights. The outer layer of the structure will have a height of 1.8 m with lengths up to 200 m. The second layer will be positioned in the centre of the AFA at a height of 3 m and a length of 100 m on each side. The second layer exceeds the Mean Sea Level (MSL) elevation and will be visible during low tide. Hopefully, it will provide an aesthetically pleasing feature.

4.4.3 Scenario 3

The third scenario was arranged in a square shape with a length of 100 m on each side. The design is like the second scenario. Still, without the first layer, the design eliminates the outermost, massive first layer and retains only the second layer. The height of the structure exceeds the Mean Sea Level (MSL). Figure

8 visualises the third scenario.

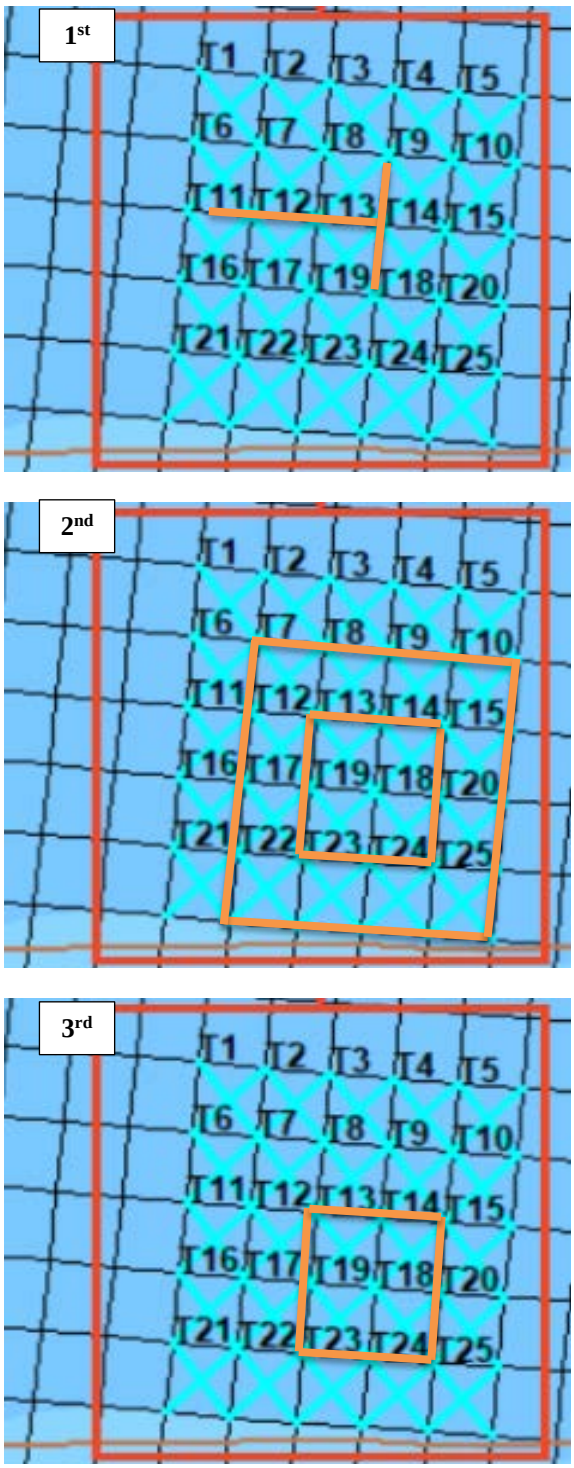

Fig. 7 Layout Configuration of Artificial Fish Apartment Each Scenarios

4.5 Analysis of Reflection Coefficient Due to Porosity of AFA Structure

In calculating the reflection coefficient, we have to determine the structure's porosity by evaluating its volumetric flow obstruction. This involves precisely calculating the fluid volume ratio to the structure's total volume. The porosity calculation follows the formula proposed by Mancheno in their 2021 research [33]. Based on the formula, Table 5 shows the obstructed fluid volume compared to the total volume. According to the table, porosity of AFA with an outer side length of 60 cm and an inner side length of 44 cm is 0.6.

Table 5. Calculation Structure Porosity

Unit	Value	Unit
Radius	104 cm	Cm
Concrete Width	8 cm	Cm
Water Volume	131.648	Cm^3
n (porosity)	0.61	-

It was found that there is a relationship between wave steepness, which refers to the wave's slope, and the wave reflection coefficient for solid structures. The measurement of wave steepness is based on the waves in front of the planned structure at Tirang Beach. Experiments involving different widths of submerged structure peaks had minimal influence on the change in Kr values. As a result, the porous structure's reflection coefficient values in each structure construction scenario can be seen in Table 6.

Table 6. Reflection Coefficient

Scenario	1	2		3
Kr_{solid}	0.28	0.3	0.28	0.28
Kr_{porous}	0.19	0.2	0.19	0.19

By knowing the reflection coefficient values for solid structures, the reflection coefficient for the porous structure can be determined. The determination of the reflection coefficient for the porous structure is based on previous research conducted by Chyon in 2017 [34]. In their study, Chyon established a relationship between the reflection coefficients for porous and solid structures based on the porosity values (n) as calculated earlier. The porosity value for a solid structure is 0 since it does not allow water or sediment to pass through [34].

4.6 Analysis of Transmission Coefficient Due to Porosity of AFA Structure

The porous AFA structure is designed with cavities to allow wave transmission and reduce wave energy. The wave transmission coefficient represents the wave reduction caused by the presence of the porous AFA structure. The structure reflects waves on its solid parts while reducing the incoming sea waves through the cavities present in the AFA structure. The magnitude of wave reduction caused by the AFA structure can be analysed through the

value of the transmission coefficient, where a smaller transmission coefficient indicates a more significant contribution of the AFA structure in wave reduction.

The transmission coefficient is obtained by considering the transmission coefficient of the porous or cavity structure and the structure's coefficient in fully submerged conditions. The submerged transmission coefficient is obtained with utmost precision by modelling the AFA structure using the advanced Delft3D. Calculations from previous analyses are incorporated as parameters in the wave modelling to determine the transmission coefficient of the embedded structure for each modelling scenario. Table 7 shows the transmission coefficient that is used.

Table 7. Transmission Coefficient

Scenario	1		2	3
Kt_{porous}	0.88	0.33	0.88	0.88
$Kt_{submerged}$	0.16	0.42	0.16	0.16
Kt_{final}	0.14	0.14	0.14	0.14

The values of α and β are selected to correspond to the shape of the DAM structure, with an assumed value of α = 2.6 and β = 0.15. Furthermore, the width of the modified AFA structure (B) will be determined as 1.2 m.

4.7 Analysis of Erosion and Sedimentation

The analysis of the AFA structure modification can be observed explicitly by modelling the conditions of Tirang Beach, incorporating the structural parameters placed at specific locations within the observation points in the conducted modelling. In the modelling, there are 25 observation points spread along the coastline of Tirang Beach, where the erosion and sedimentation conditions in the existing state can be examined for each point.

These scenarios can be visualized through time series graphs, depicting the changes in erosion and sedimentation over time. Figure 8-12 shows the results of erosion and sedimentation for the fourth row of observation points at T16 until T20. The row from T16 to T20 is selected as the main observation location because it is anticipated to have the highest sedimentation in front of Tirang Beach. Sedimentation or erosion at another point have a lower a result than T16 to T20.

The model was conducted for three months and the data was shown each 2 weeks. Based on the analysis, scenario 2 has the highest result in T16, T17, T18 and T19. Meanwhile, in T20, the first scenario gets the highest results.

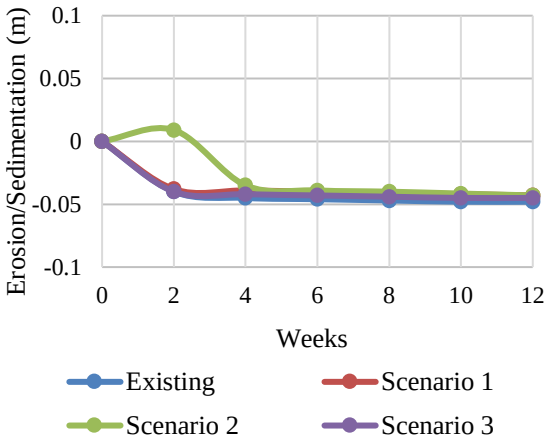

Fig. 8 Graphic of Erosion and Sedimentation at Observation Point T16

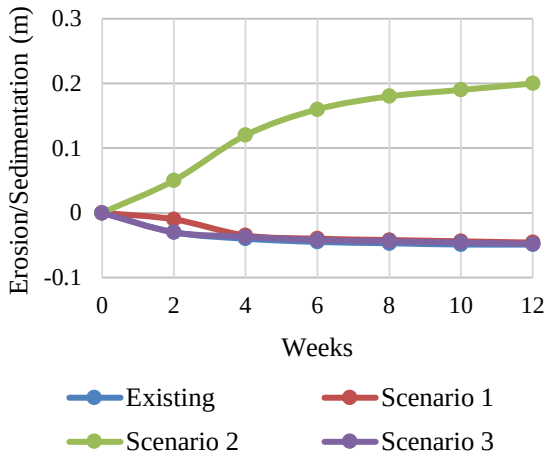

Fig. 9 Graphic of Erosion and Sedimentation at Observation Point T17

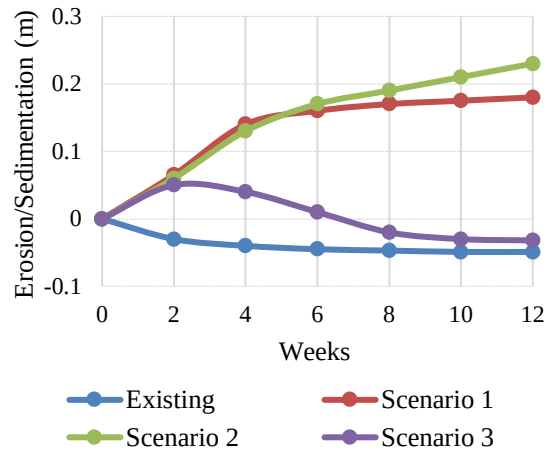

Fig. 10 Graphic of Erosion and Sedimentation at Observation Point T18

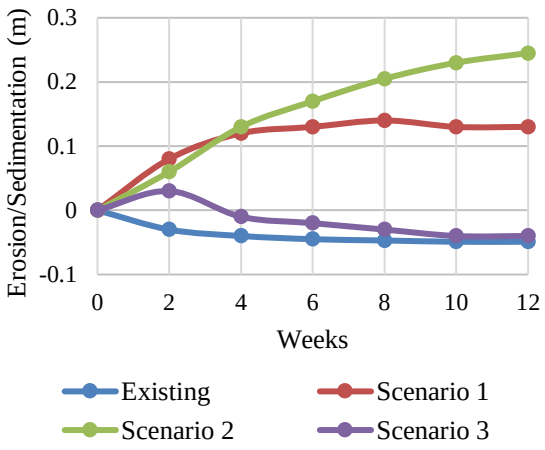

Fig. 11 Graphic of Erosion and Sedimentation at Observation Point T19

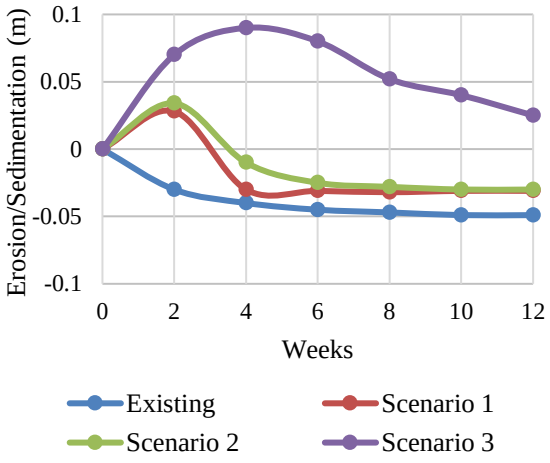

Fig. 12 Graphic of Erosion and Sedimentation at Observation Point T20

Observation points T17 - T19 in scenario two experience significant sedimentation of up to 0.25 m due to the increased height of the second layer structure, resulting in a higher sediment trapping capability. In scenario 3, sedimentation reaches 0.17 m, resulting in an increase of approximately 0.22 m from the initial elevation of - 0.05 m. If scenario 2 exhibits an increase of 0.28 m, there is a difference of 0.05 m between scenarios 2 and 3.

According to the model results from observation points, sedimentation in the first scenario ensues at T20, with the sediment high at less than 5 cm. The second scenario gets the highest result. The sedimentation takes place at 12 observation points. The accumulation of sediment reached 30 cm at observation point T13. In the third scenario, sediment settles at 4 locations, with the highest accumulation reaching 17 cm at T19. Figure 13 depicts the sedimentation and erosion at each observation point.

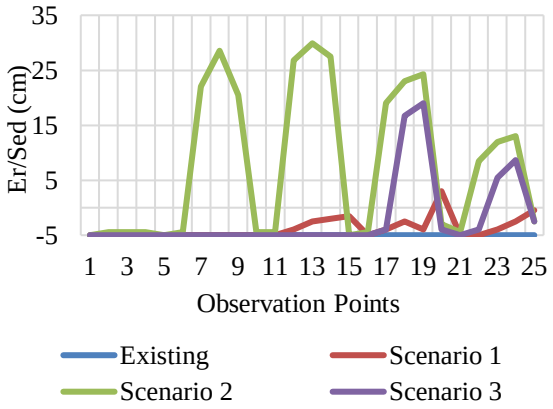

Fig. 13 Graphic of Cumulative Erosion and Sedimentation at Each Observation Points

Based on Fig. 13, the results indicate that scenario 2 has the best impact on land emergence. This is evident from the significant sedimentation values observed in each row. This scenario has the highest sedimentation and occurs at 12 of 25 observation points.

4.8 Changes in Seabed Elevation

The analysis of the AFA structure modification can be observed explicitly by modelling the conditions of Tirang Beach, incorporating the structural parameters placed at specific locations within the observation points in the conducted modelling. In the modelling, there are 25 observation points spread along the coastline of Tirang Beach, where the erosion and sedimentation conditions in the existing state can be examined for each point. These scenarios can be visualized through time series graphs, depicting the changes in erosion and sedimentation over time.

As previously modelled, Tirang Beach's current seabed condition experiences erosion and decreased coastal seabed elevation. Changes in the seabed elevation align with the modelling of erosion and sedimentation, which can be observed at each designated observation point mentioned earlier as seen at Figure 14 – 18.

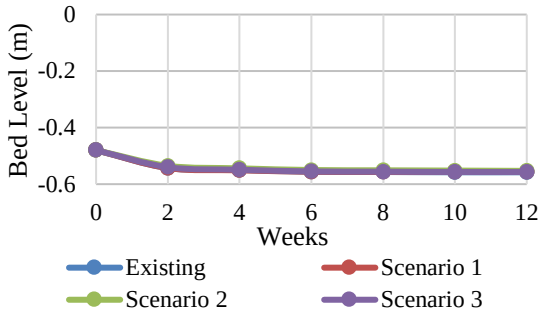

Fig. 14 Graphic of Changes in Seabed Elevation at Observation Point 16

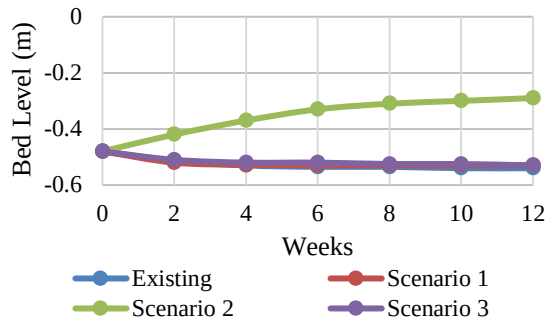

Fig. 15 Graphic of Changes in Seabed Elevation at Observation Point 17

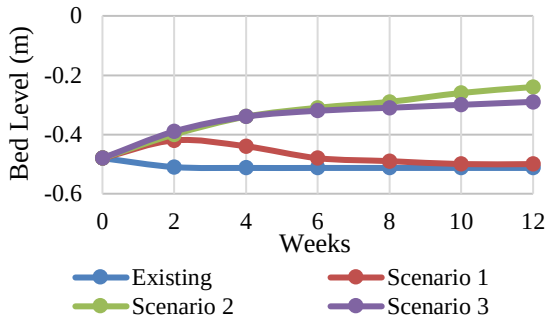

Fig. 16 Graphic of Changes in Seabed Elevation at Observation Point 18

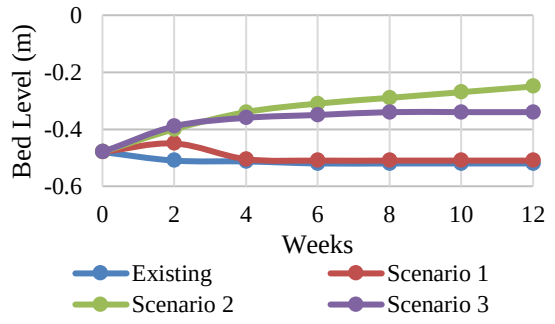

Fig. 17 Graphic of Changes in Seabed Elevation at Observation Point 19

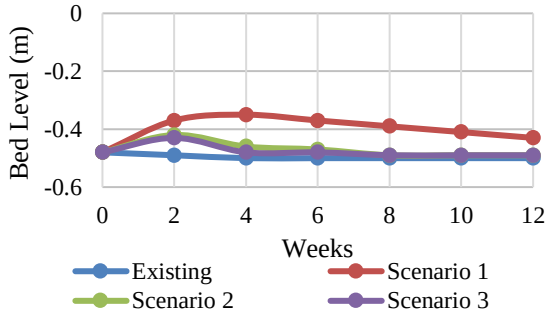

Fig. 18 Graphic of Changes in Seabed Elevation at Observation Point 20

Implementing the modified AFA structure as a coastal protection measure against incoming large waves from the sea and to calm the waters in front of the beach can effectively deposit sediments. Scenarios that result in the most significant increase in seabed elevation will significantly reduce erosion or even facilitate sedimentation in certain conditions.

According to the graph, there is a substantial increase in seabed elevation due to significant sedimentation, with the highest increase reaching an elevation of -0.25 m. This represents a change of approximately 0.25 m compared to the previous elevation of -0.55 m. This occurs primarily because scenario 2 involves layered structures, allowing for gradual and more effective wave reduction, resulting in calmer waters and increased sediment deposition. However, at observation point T20, which is on edge, the direction of the wave from the northwest has already deposited most of the sediment at other points in scenario 2. As a result, T20 does not exhibit a significant increase in elevation.

Table 8. Maximum Changes in Seabed Elevation

	Deviation (m)				
50	0.006	0.126	0.161	0.165	0.024
100	0.004	0.242	0.274	0.287	0.018
150	0.003	0.317	0.347	0.325	0.012
200	0.002	0.264	0.335	0.256	0.004
250	0.001	0.002	0.002	0.002	0.001

Analysis of the seabed elevation is shown in Figure 19 - 23. The second scenario on the graph obtains the most significant changes, with a maximum increase of 0.35 m in the seabed elevation within three months. The wave reduction is already at its maximum for T16 - T19. Table 8 describes the maximum changes in seabed elevation.

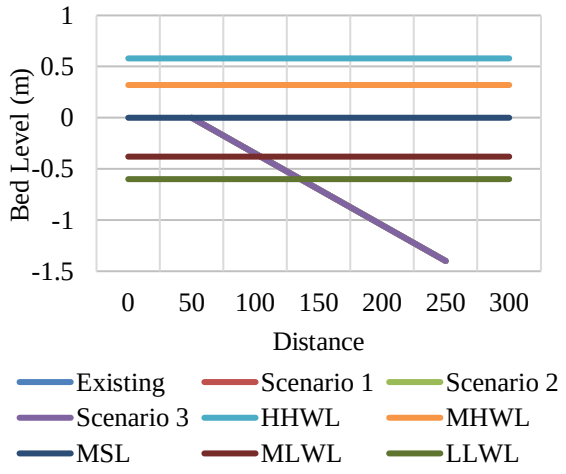

Fig. 19 Seabed Cross-Section Profile 1

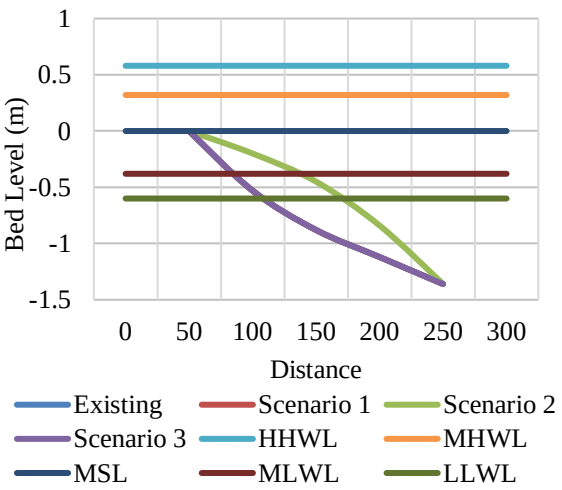

Fig. 20 Seabed Cross-Section Profile 2

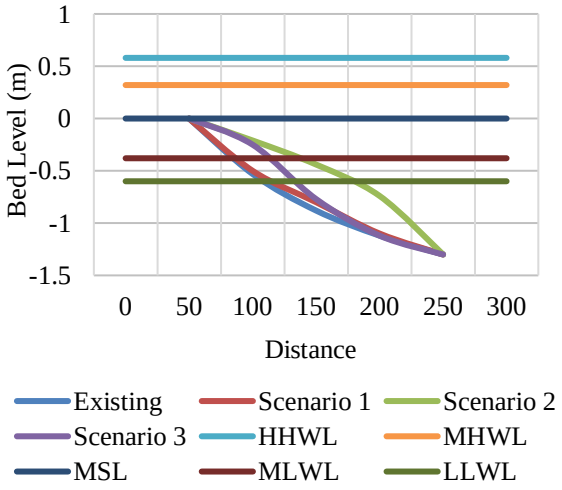

Fig. 21 Seabed Cross-Section Profile 3

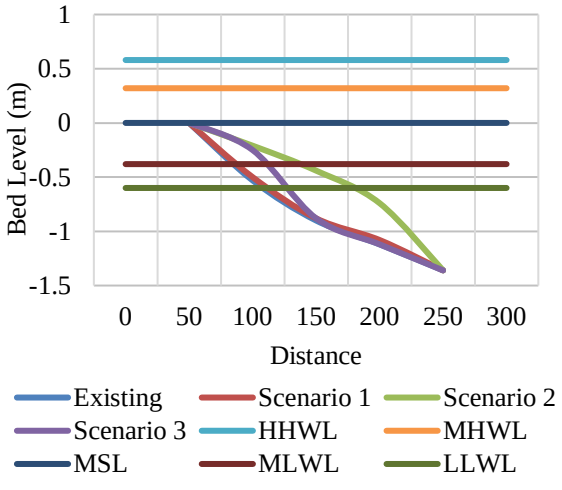

Fig. 22 Seabed Cross-Section Profile 4

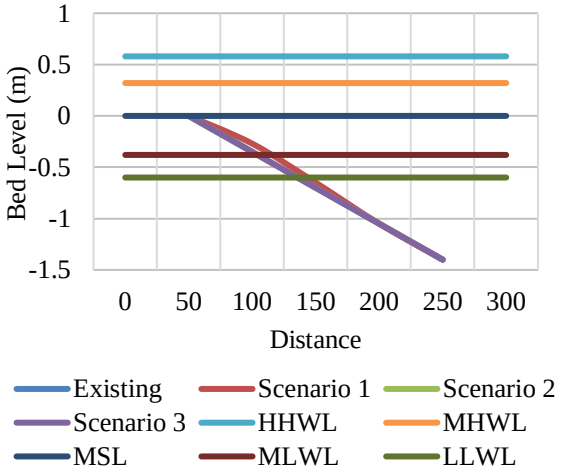

Fig. 23 Seabed Cross-Section Profile 5

In the first scenario, at observation point T20, the substantial sediment capture is a testament to the effectiveness of our data collection methods, leading to a maximum seabed elevation increase of 0.09 m at this location. In the first scenario, elevation increased up to -0.3 m from -0.51 m, resulting in a rise of 0.21 m.

Consequently, from the most profound seabed elevation of -1.4 m, reaching the Mean Sea Level (MSL) elevation and emerging new land can be predicted to occur in approximately four years. Achieving the High Highest Water Level (HHWL) condition at an elevation of 0.59 m would require approximately 5.7 years. For scenario 3, it would take six years to reach the Mean Sea Level (MSL) elevation and for land to emerge. Scenario 2 would take approximately 5.7 years to get the Highest High-Water Level (HHWL) of 0.59 m, whereas scenario three would require nine years to achieve the same HHWL elevation.

4.9 Analysis of Wave Reduction Due to the Structure

As previously known, Tirang Beach experiences significant erosion or abrasion due to destructive ocean waves. Therefore, analyzing the wave reduction caused by the Artificial Fish Apartment (AFA) protective structure becomes crucial.

The higher the reduction in wave height, the lower the wave energy in the waters surrounding Tirang Beach, which positively impacts desired sedimentation events. This analysis, which will be conducted with a comprehensive approach, will involve examining the maximum wave heights during the modelling period and comparing them with the existing conditions and all structural scenarios.

Figures 24 highlight a crucial finding. The second scenario demonstrates the most significant wave reduction. In scenario 1, the reduction is uneven, sometimes approaching zero, resulting in the absence

of formed waves. The average wave reduction calculation shows that the second scenario outperforms the existing conditions with a reduction of 0.3 m. In contrast, scenarios 1 and 3 show a slightly lower reduction of approximately 0.12 m, while scenario 2 reduces wave height of less than 0.1 m. These findings are of paramount importance in understanding wave reduction scenarios.

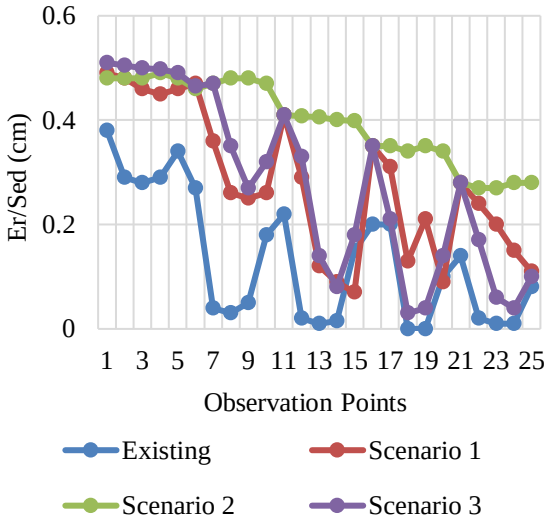

Fig. 24 Wave Reduction Graph for Each Observation Points

Table 9 compares wave reduction in front of structures in every scenario. The calculation of reduction in wave height before and after the structural scenario shows scenario 2 has the highest wave height reduction, with a maximum decrease of 0.26 m. In rows 1 and 2, scenario 1 has a more significant reduction. However, in rows 3, 4, and 5, scenario 3 has a more substantial impact on wave reduction.

Table 9. Significant Wave Reduction in Front of the Structure in Each Scenarios

Row	1st	2nd	3rd	Max
1	0.04	0.15	0.04	
2	0.08	0.25	0.11	
3	0.13	0.26	0.21	0.26
4	0.04	0.26	0.21	
5	0.12	0.21	0.15	

4.10 Determining the Best Alternative

The author utilizes the Analytic Hierarchy Process (AHP) method to determine the best alternative. This decision-support model breaks down complex multi-factor or multi-criteria problems into a hierarchy [35]. The evaluation criteria for the modified AFA structure include seven criteria, as seen in Table 10.

Table 10. Criteria Assessment for Structural Scenarios

No	Criteria
1	Implications of Erosion Mitigation or Sedimentation Enhancement
2	Aesthetic Considerations
3	Construction, Operational, and Maintenance Costs
4	Challenges in Construction
5	Transformation into a New Fish Habitat
6	Development as a Tourist Attraction
7	Environmental Consequences

In this case, AHP is used with multiple evaluation criteria using a fuzzy scale to determine the values between aspects and towards the alternative AFA structure scenarios. After evaluating each scenario's structure according to each criterion, the obtained scores are multiplied by the weight of each criterion. Thus, the results of the AHP evaluation indicate that out of the three available scenarios, scenario 2 has the highest weight and is recommended as the top priority, with a score of 43%. The second-ranked scenario is scenario 5, with a score of 20%.

5. CONCLUSION

The analysis conducted at Tirang Beach shows the importance of coastal protection, especially in the form of artificial fish apartments, which aim to secure and create new sediment land areas. Wave hindcasting was performed using the SPM-1984 method, with the most dominant wave direction coming from the northwest, a significant wave height of 0.9 m, and a considerable wave period of 3.72 m. The analysis of the conditions at Tirang Beach revealed a maximum erosion of 4.84 centimetres and a sea-level change of -1.4 m. The study of the structural modelling, which examined erosion and sedimentation resulting from the construction of the modified artificial fish apartment (AFA) structure, indicates that scenario two positively impacts the emergence of new land. The analysis of each row shows that scenario 2 is the most favourable, with a maximum sedimentation of 0.3 m.

In scenario 2, the seabed elevation undergoes the most significant changes, with a maximum increase of 0.35 m within three months. Thus, starting from the most profound seabed elevation of -1.4 m, it is predicted that it will take approximately four years to reach Mean Sea Level (MSL). Achieving the Highest High Water Level (HHWL) condition at an elevation of 0.59 m would take approximately 5.7 years. Scenario 2 shows the best and most significant

reduction in the maximum wave height, with a maximum decrease of 0.26 m observed from the location through the structure. Compared to the existing condition, the average calculated wave height reduction in the scenario is approximately 0.3 m. In contrast, other scenarios demonstrate a smaller decrease of around 0.12 m.

The Analytic Hierarchy Process (AHP) method was employed to determine the best alternatives. The results of the AHP assessment indicate that among the three available scenarios, scenario two is highly recommended as the top priority, with a score of 48%, followed by scenario 5 in second place with a score of 21%.

6. NOMENCLATURE

Kr	Reflection coefficient	
Hr	Wave height after reflection	(m)
Hi	Wave height that is coming (m)	
Er	Energy of reflection	
Ei	Energy of the coming wave	
Kt	Transmission coefficient	
Ht	Wave height after passing the structure (m)	
Hi	Wave height that is coming	(m)
Et	Energy of transmission	
Rc	Freeboard height	(h – d)
d	Average water level height relative to the reference level	
α, β	Structure type coefficients	
Feff	Fetch effective	
Fi	The length of the fetch to I	(m)
cos α	Fetch angle to I	(^{0})

7. ACKNOWLEDGMENTS

The authors would like to acknowledge the contribution of PPMI 2023 for funding this research and Oceanography Department of Diponegoro University, Indonesia for their support in term of field data sharing and valuable discussion during the research.

8. REFERENCE

[1] Djunarsjah E and Putra A. P., The concept of an Archipelagic Province in Indonesia. IOP Conference Series: Earth and Environmental Science, Vol. 777, Issue. 1, 2021, pp. 12040-12047.

[2] Chen H., Tang L., Qiu Q., Hou L., and Wang B., Construction and Case Analysis of an Index for The Sustainability of Ecosystem Services. Ecological Indicators, Vol. 115, 2020, pp. 106370-106381.

[3] Utama D.R., Hamsal M., Abdinagoro S.B., and Rahim R.K., Developing A Digital Transformation Maturity Model for Port Assessment in Archipelago Countries: The Indonesian Case. Transportation Research Interdisciplinary Perspectives, Vol. 26, 2024, pp. 101146-101162.

[4] Göktürk O.M., Sobolowski S.P., Simon M.H., Zhang Z., and Jansen E., Sensitivity Of Coastal Southern African Climate To Changes In Coastline Position And Associated Land Extent Over The Last Glacial', Quaternary Science Reviews, Vol. 300, 2023, pp. 107893-107903.

[5] Nevermann H., Gomez J.N.B., Fröhle P., and Shokri N., Land Loss Implications Of Sea Level Rise Along The Coastline Of Colombia Under Different Climate Change Scenarios. Climate Risk Management, Vol. 39, 2023 pp. 100470-101479.

[6] Harley M.D. and Kinsela M.A., Coastsnap: A Global Citizen Science Program To Monitor Changing Coastlines. Continental Shelf Research, Vol. 245, 2022, pp. 104796-104808.

[7] Dewi R.S. and Bijker W., Dynamics Of Shoreline Changes In The Coastal Region Of Sayung, Indonesia. The Egyptian Journal Of Remote Sensing and Space Science, Vol. 23, Issue. 2, 2020, pp. 181–193.

[8] Khakhim N., Kurniawan A., Pranowo W.S., Khasanah E.U., and Halilintar P., Shoreline Morphological Change Prognostic Model Based On Spatiotemporal Framework Imagery Data On The Northern Coast Of Java, Indonesia. Kuwait Journal Of Science, Vol. 51, Issue. 4, 2024, pp. 100274-100287.

[9] Yamamoto Y., Living Under Ecosystem Degradation: Evidence From The Mangrove–Fishery Linkage In Indonesia. Journal of Environmental Economics and Management, Vol. 118, 2023, pp. 102788-102810.

[10] Lemos G., Bosnic I., Antunes C., Vousdoukas M., Mentaschi L., and Soares P.M.M., The Future Of The Portuguese (Sw Europe) Most Vulnerable Coastal Areas Under Climate Change – Part I: Performance Evaluation And Shoreline Evolution From A Downscaled Bias Corrected Wave Climate Ensemble. Ocean Engineering, Vol. 302, 2024, pp. 117661-117680.

[11] Spencer N., Strobl E., and Campbell A., Sea Level Rise Under Climate Change: Implications For Beach Tourism In The Caribbean. Ocean and Coastal Management, Vol. 225, 2022, pp. 106207-106222.

[12] Bott L.M., Schöne T., Illigner J., Haghighi M.H., Gisevius K., and Braun B., Land Subsidence In Jakarta And Semarang Bay – The Relationship Between Physical Processes, Risk Perception, And Household Adaptation. Ocean and Coastal Management, Vol. 211, 2021, pp. 105775-105786.

[13] Barco M.K.D., Furlan E., Pham H.V., Toressan S., Zachopoulos K., Kokkos N., Sylaios G., Critto A., Multi-Scenario Analysis In The Apulia Shoreline: A Multi-Tiers Analytical Framework For The Combined Evaluation And Management Of Coastal Erosion And Water Quality Risks. Environmental Science and Policy, Vol. 153, 2024, pp. 103665-103679.

[14] Dong W.S., Ismailluddin A., Yun L.S., Ariffin E.H., Saengsupavanich C., Maulud K.N.A., Ramli M.Z., Miskon M.F., Jeofry M.H., Mohamed J., Mohd F.A., Hamzah S.B., Yunus K., The Impact Of Climate Change On Coastal Erosion In Southeast Asia And The Compelling Need To Establish Robust Adaptation Strategies. Heliyon, Vol. 10, Issue. 4, 2024, pp. e25609 (20 pages).

[15] Humphries U. and Kaewmesri P., The Performance Sea Surface Temperature Anomaly Over Pacific Ocean And Niño 3.4 Area By Using Intermediate Coupled Model (ICM). International Journal of Geomate, Vol. 21, Issue. 84, 2021, pp. 228–235.

[16] Bumi I.S., Widyaningtias, and Adityawan M. B., Coastal Erosion Management By Implementing Concept Of Building With Nature (BwN) In Demak Regency, Central Java, Indonesia. IOP Conference Series: Earth and Environmental Science, Vol. 698, Issue. 1, 2021 pp. 12005-12011.

[17] Zhang Y., Ouyang Z., Xu C., Wu T., and Lu F., A Multi-Hazard Framework For Coastal Vulnerability Assessment And Climate-Change Adaptation Planning. Environmental and Sustainability Indicators, Vol. 21, 2024, pp. 100327-100335.

[18] Esteban M., Takagi H., Jamero L., Chadwick C., Avelino J.E., Mikami T., Fatma D., Yamamoto L., Thao N.D., Onuki M., Woodbury J., Valenzuela V.B., Crichton R.N., Shibamaya T., Adaptation To Sea Level Rise: Learning From Present Examples Of Land Subsidence. Ocean and Coastal Management, Vol. 189, 2020, pp. 104852-104862.

[19] Widyaningtias, Bumi I.S., Adityawan M.B., Nugroho J., and Kuntoro A. A., Implementation Of Building With Nature (BwN) As Adaptive Concept To Prevent Coastal Erosion In Demak Regency, Central Java, Indonesia. International Journal on Advance Science Engineering Information Technology, Vol. 12, Issue. 5, 2022, pp. 2023–2029.

[20] Arif D.A., Prarikeslan W. and Syaharani L., Analysis Of Shoreline Dynamics For Coastal Management Practice In Pariaman, West Sumatera, International Journal of Geomate, Vol. 19, Issue. 72, 2020, pp. 166–172.

[21] Magdale I., Suhardi J.L.E., and Adityawan M.B., Analytical And Numerical Studies For The Reduction Of Wave Run-Up Height By A Submerged Breakwater. International Journal of Geomate, Vol. 20, Issue. 77, 2021, pp. 1–9.

[22] Sanusi N.A., Ghazali N.A., Alipiah R.M., Koris R., and Zakariya R., Survey Dataset On Socioeconomic Status And Artificial Reef Fishing Activity On Terengganu Coastal Water. Data In Brief, Vol. 52, 2024, pp. 110028-110038.

[23] Iqbal M., Widyaningtias, Wiyono A., Adityawan M.B., Sukarno I., and Bumi I.S., Effect Of Permeable Structure On Coastal Sediment Transport In Demak Regency, Central Java, Indonesia Model By Using Delft3D Software. IOP Conference Series: Earth and Environmental Science, Vol. 698, Issue. 1, 2021, pp. 12040-12046.

[24] Carral L., Lamas M.I., Barros J.J.C., López I., and Carballo R., Proposed Conceptual Framework To Design Artificial Reefs Based On Particular Ecosystem Ecology Traits. Biology, Vol. 11, Issue. 5, 2022, pp. 680-699.

[25] Zanin G.M., Muwafu S.P., and Costa M.M., Nature-Based Solutions For Coastal Risk Management In The Mediterranean Basin: A Literature Review. Journal Of Environmental Management, Vol. 356, 2024, pp. 120667-120676.

[26] Díaz-Carrasco P., Eldrup M.R., and Andersen T.L., Advance In Wave Reflection Estimation For Rubble Mound Breakwaters: The Importance Of The Relative Water Depth. Coastal Engineering, Vol. 168, 2021, pp. 103921-103933.

[27] Díaz-Carrasco P., Molines J., Gómez-Martín M. E., and Medina J.R., Simple And Explicit Neural Network-Derived Formula To Estimate Wave Reflection On Mound Breakwaters. Coastal Engineering, Vol. 186, 2023, pp. 104404-1044016.

[28] Gong Q., Jiang M.-T., Pang C.-L., Zhang X.-J., Chen X.-Y., and Ni Y.-L., Wave Energy Reflection By The Bragg Breakwater Composed Of Rectangular Bars On The Horizontal Permeable Seabed. Energy Reports, Vol. 8, 2022, Pp. 566–573.

[29] Muliati Y., Tawekal R. L., Wurjanto A., Kelvin J., and Pranowo W. S., Wind Wave Modeling In Natuna Sea: A Comparison Among Swan, Seafine, And Era-Interim. International Journal of Geomate, Vol. 16, Issue. 54, 2019, pp. 176–184.

[30] Peñaloza-Gutierrez J. J., Tejada-Martínez A. E., and Boufadel M. C., Reynolds-Averaged Navier-Stokes Simulation Of Nearshore Langmuir Circulation And The Formation Of Oil-Particle Aggregates. Ocean Modelling, Vol. 187, 2024, pp. 102306-102318.

[31] Morgan J. A., Kumar N., Horner-Devine A. R., Ahrendt S., Istanbullouglu E., and Bandaragoda C., The Use Of A Morphological Acceleration Factor In The Simulation Of Large-Scale Fluvial Morphodynamics. Geomorphology, Vol. 356, 2020, pp. 107088-107100.

[32] Ormondt M.V., Nelson T.R., Hapke C.J., and Roelvink D., Morphodynamic Modelling Of The Wilderness Breach, Fire Island, New York. Part I: Model Set-Up And Validation. Coastal Engineering, Vol. 157, 2020, pp. 103621-103635.

[33] Mancheño A.G., Jansen W., Winterwerp J.C., and Uijttewaal W.S.J., Predictive Model Of Bulk Drag Coefficient For A Nature-Based Structure Exposed To Currents. Scientific Reports, Vol. 11, Issue. 1, 2021, pp. 3517-3530.

[34] Chyon Md. S. A., Rahman A., and Rahman Md. A., Comparative Study On Hydrodynamic Performance Of Porous And Non-Porous Submerged Breakwater. Procedia Engineering, Vol. 194, 2017, pp. 203–210.

[35] Soetjipto J.W., Hidayah E., Dewi A.L., Widiarti W.Y., and Juliastuti. An Approach For Irrigation Network Rehabilitation Priority Based On Hybrid AHP-TOPSIS, Waspas, Moora. International Journal of Geomate, Vol. 25, Issue. 110, 2023, pp. 49–58.